REPORT DOCUMENTATION PAGE

Form Approved
OMB No. 0704-0188

1. AGENCY USE ONLY *(Leave blank)*	2. REPORT DATE	3. REPORT TYPE AND DATES COVERED
		Final Report

4. TITLE AND SUBTITLE
A New Approach for Combined Epitaxial Metallization and Heavy Doping of Shallow Junctions

5. FUNDING NUMBERS

6. AUTHOR(S)
M.A. Hasan

7. PERFORMING ORGANIZATION NAME(S) AND ADDRESS(ES)
Dept. of electrical and Computer Engineering & C.C. Cameron Applied Research Center, The University of North Carolina, Charlotte

8. PERFORMING ORGANIZATION REPORT NUMBER
41103-MS

9. SPONSORING/MONITORING AGENCY NAME(S) AND ADDRESS(ES)
U.S. Army Research Office
P.O. Box 12211
Research Triangle Park, NC 27709-2211

10. SPONSORING/MONITORING AGENCY REPORT NUMBER

11. SUPPLEMENTARY NOTES
The views, opinions and/or findings contained in this report are those of the author and should not be construed as an official Department of the Army position, policy or decision, unless so designated by other documents.

12a. DISTRIBUTION AVAILABILITY STATEMENT
Approved for public release; distribution unlimited.

12b. DISTRIBUTION CODE

13. ABSTRACT *(Maximum 200 words)*
This short-term innovative research project investigated the epitaxial growth of silicon deposited from the vapor phase onto an Al-covered silicon substrate. The 60 nm Al layer behaved as if it were transparent to the Si flux. The silicon cleanly passed through the Al layer to the buried Al/Si interface where it formed a defect-free Si layer on the original single crystal Si substrate. The new growth method is referred to as solid-metal mediated molecular beam epitaxy (SMM-MBE). Most of the work focused on Si(111), but some initial results were also obtained for Si(100).

14. SUBJECT TERMS	15. NUMBER OF PAGES
Solid-metal mediated molecular beam epitaxy (SMM-MBE)	20
	16. PRICE CODE

17. SECURITY CLASSIFICATION OF REPORT	18. SECURITY CLASSIFICATION OF THIS PAGE	19. SECURITY CLASSIFICATION OF ABSTRACT	20. LIMITATION OF ABSTRACT
unclassified	unclassified	unclassified	

Final Report

Project Number 2000-0175

A New Approach for Combined Epitaxial Metallization and Heavy Doping of Shallow Junctions

UNCCHARLOTTE

M.-A. Hasan

The University of North Carolina at Charlotte
Department of Electrical and Computer Engineering &
C.C. Cameron Applied Research Center

TABLE OF CONTENTS

TABLE OF CONTENTS 2

I. INTRODUCTION 3

Solid-metal mediated molecular beam epitaxy (SMM-MBE) 3

II. THE MODEL SYSTEM: SMM-MBE ON SI(111) 6

II. 1. Experimental Procedure 6

II.2. Experimental Results 7

III. SMM-MBE ON SI(100) 11

IV. GROWTH OF SI ON INSULATORS (SOI) USING SMM-MBE 12

V. DOPING OF SI USING SMM-MBE 14

VI. GROWTH MECHANISM 15

REFERENCES 16

APPENDIX A 18

SYSTEM CONFIGURATION 18

I. INTRODUCTION

The goal of this project is to investigate the utilization of a new growth method, solid-metal mediated molecular beam epitaxy (SMM-MBE), in the fabrication of highly doped shallow junctions on Si together with epitaxial metal contact. In the following, a short description of SMM-MBE is given, followed by a summary of the efforts expended for the project and the results obtained. The MBE system description and experimental setup is given in Appendix A.

Solid-metal mediated molecular beam epitaxy (SMM-MBE)

A novel, low-temperature, spontaneous epitaxial growth phenomenon in which epitaxial growth from the vapor phase is conducted at a buried metal/semiconductor interface without measurable delay between the deposition on the THICK SOLID METAL surface and regrowth at the buried interface. This method is different from surfactant assisted growth. Here, the metal is THICK and SOLID unlike the case of surfactant where the thickness of the metal layer is only a fraction of a monolayer thick. This method was tested and demonstrated using Al/Si(111) as a model system. Fig. 1 schematically shows the SMM-MBE growth process. In normal MBE and for a two-layer film, the sequence of the layers follows that of the deposition order. In SMM-MBE, the second-layer grows epitaxially buried between the first layer and the substrate.

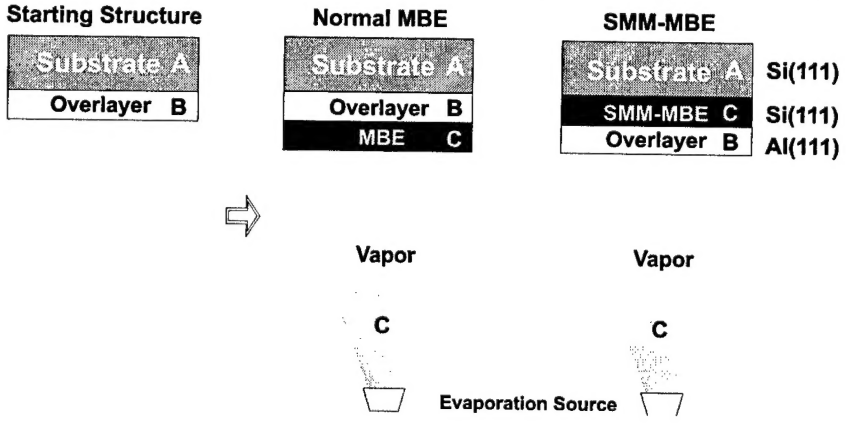

Figure 1. Schematic showing the differences between normal MBE and SMM-MBE deposition. The Al/Si system works as an excellent model for this regime of depositions.

We have demonstrated the method for Si(111) and extended the work to Si(100) under the current contract.

In this work, we have shown that Si deposited from the vapor phase on Al-coated Si substrate grew epitaxially at the buried Al/Si interface as if the Al layer was transparent to the incident flux. Most of the work was focused on Si(111), but some initial results were obtained for Si(100). SMM-MBE works on both substrates for wide range of temperatures extending from the Si/Al eutectic temperature (577 °C) down to ~ 175 °C. Detailed analytical investigation of SMM-MBE was carried out at 400 °C to insure good understanding of the results. The growth was conducted in a multi-chamber MBE system allowing for *in-situ* RHEED, LEED, and AES and with

a base pressure of ~ $5x10^{-11}$ Torr. For Si(111), the Si(111)7x7 surface was prepared by *ex-situ* chemical growth-etch-regrowth of SiO_2 followed by *insitu* thermal etch at 850 °C. Al-induced Si(111)$\sqrt{3}$x$\sqrt{3}$ was then created by depositing ~ 0.2 ML of Al at 700 °C. This step was necessary in order to insure subsequent growth of single-domain, single crystalline Al(111) layer. We will refer to this method as surface-reconstruction-induced epitaxy (SRIE). The substrate was then cooled to room temperature and Al was deposited to a thickness of 120 nm. LEED showed Al(111)1x1 surface with relatively sharp diffraction spots indicating a smooth and well ordered Al(111) surface. The substrate temperature was elevated to 400°C and a 60-nm-thick Si layer was grown using a growth rate of 1 Å s^{-1}. AES analysis after growth of Si showed mainly Al peak while LEED showed no change in the diffraction pattern. These results indicate in-diffusion of Si through the single crystalline Al(111) layer with no structural changes in the Al overlayer. TEM investigations, while confirming the epitaxial relationship between Al(111) and Si(111), showed the formation of defect-free, epitaxial Si(111) at the Al(111)/Si interface. The thickness of the epitaxial Si(111) layer is equivalent to the total deposited Si flux. The Al/Si interface was abrupt and similar to those grown without solid-metal mediated MBE indicating minimal intermixing. The Al-mediated epitaxy of Si is explained in terms of high Si diffusivity in Al, low solid solubility of Si in Al, and the absence of Al-Si intermetallic compounds. SMM epitaxial growth then occurs through epitaxial accommodation of diffusing Si atoms at the buried Si(111) surface. The absence of strong Si AES signal at the Al surface after Si deposition indicates that mass transport through the Al layer is larger than the Si deposition rate which was 1 Å s^{-1}. Similar results were obtained for growth temperatures between ~ 175 and 550 °C

For Si(100), similar procedures, except for the SRIE step, were followed and buried growth using SMM-MBE was obtained.

In the following sections, a short historical account of related methods and description of the obtained results will be given.

Historical Background

Figure 2 differentiate between this method and its historical antecedents. In 1964, Wagner and Ellis[1,2] reported epitaxial growth of single-crystalline Si using liquid Au as a mediator during vapor phase deposition. Si whisker growth was realized because of using chemical compound vapor instead of a pure source and the lack of now established Si-surface cleaning methods. This technique is currently used by a Russian group to grow Si whiskers for use as field emitters. Later in 1991, Xiong et. al [3] using more advanced vacuum and cleaning procedures reported planar epitaxy of Ge using the same method (liquid Au mediated). They called this method vapor-liquid-solid or liquid-metal mediated epitaxy. Typically, they used a growth rate of 0.017-0.04 nm/s and added 20 minutes annealing time after deposition to optimize the growth.

Another observation of similar nature, but using solid phase epitaxy (SPE) was reported by Majni and Ottaviani [4] in 1977. In this case, polycrystalline Al was deposited first followed by an amorphous Si layer and the whole structure was annealed for ~10 hrs at temperatures between 450 and 530 °C. They reported transport of Si through the Al layer toward the Al/Si interface. Later, Tsaur et.al [5] reported similar results for annealing time of 4 hrs at 400 °C and 30 min. at 500 °C. However, no clear information on the crystal structure and Al/Si interfaces

were reported. The RBS results reported had a high backscattering yield (compared to that of Si wafer) even at the near-interface area, indicating a considerable defect density in the regrown Si layer. For other metals, Lau et. al [6] reported formation of crystalline silicide layers using a-Si/metal/c-Si structures (metal = Pt, Fe, Pd, Cr, Co, Ti, V, and Rh) and a limited thickness of Si SPE at the original interface. Since then, a large number of reports on metal-enhanced solid phase epitaxy were reported in the literature [7] (mainly using a minute amount of metal at the a-Si/c-Si interface).

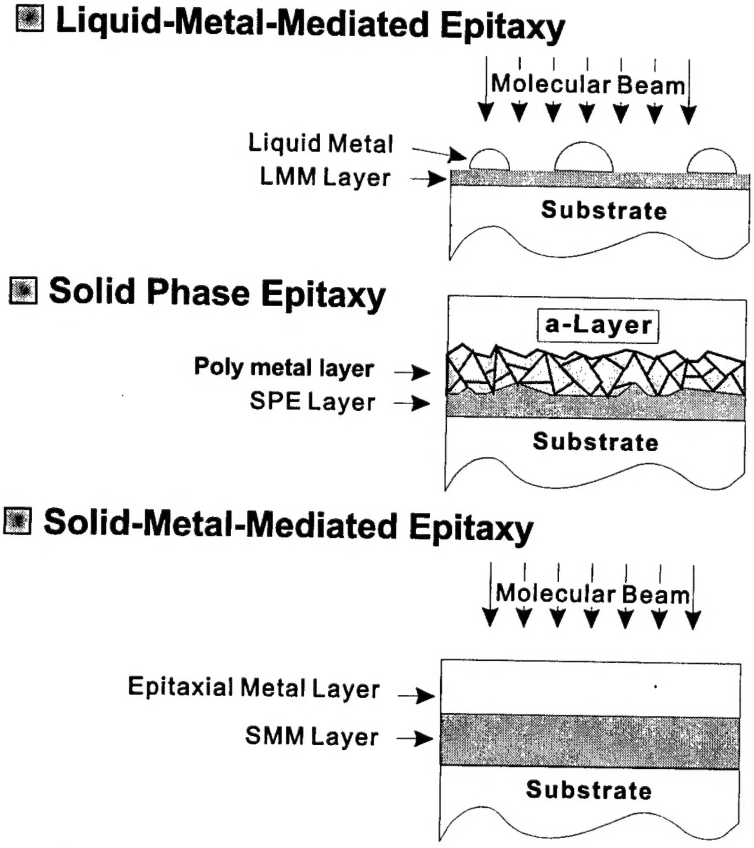

Figure 2 Schematic showing the similarities between SMM-MBE and earlier methods.

In our work, the Si growth rate from the vapor phase equaled the regrowth rate at the interface. To our knowledge, this is the first report of spontaneous growth of this sort. The Si growth rate used, which was 0.1-0.2 nm/s, is much higher than those reported using other methods and due to the spontaneous nature of growth, is compatible with mass production and processing of Si devices (0.2 nm/s = 0.72 μm/hr). The results shown here were taken from as-grown samples without any additional heat treatment. Also, there is no measurable change in the crystal quality of the single-crystalline Al layer. Single crystalline Al layers have the highest electromigration resistance reported so far [8] which enhance the reliability and lifetime of low-resistance Al interconnect layers. The cross- sectional TEM image also shows an abrupt Al/Si interface which remained stable after increasing the temperature to 400 ^{o}C and after the massive Si diffusion during the SMM

process. The abruptness and stability of the epitaxial Al/Si interface is critical for shallow junctions in order to avoid junction spiking.

II. THE MODEL SYSTEM: SMM-MBE ON Si(111)

II. 1. Experimental Procedure

Deposition for this experiment was carried out following the sequence of depositions described below (the temperature profile used during growth is shown in Figure 3):

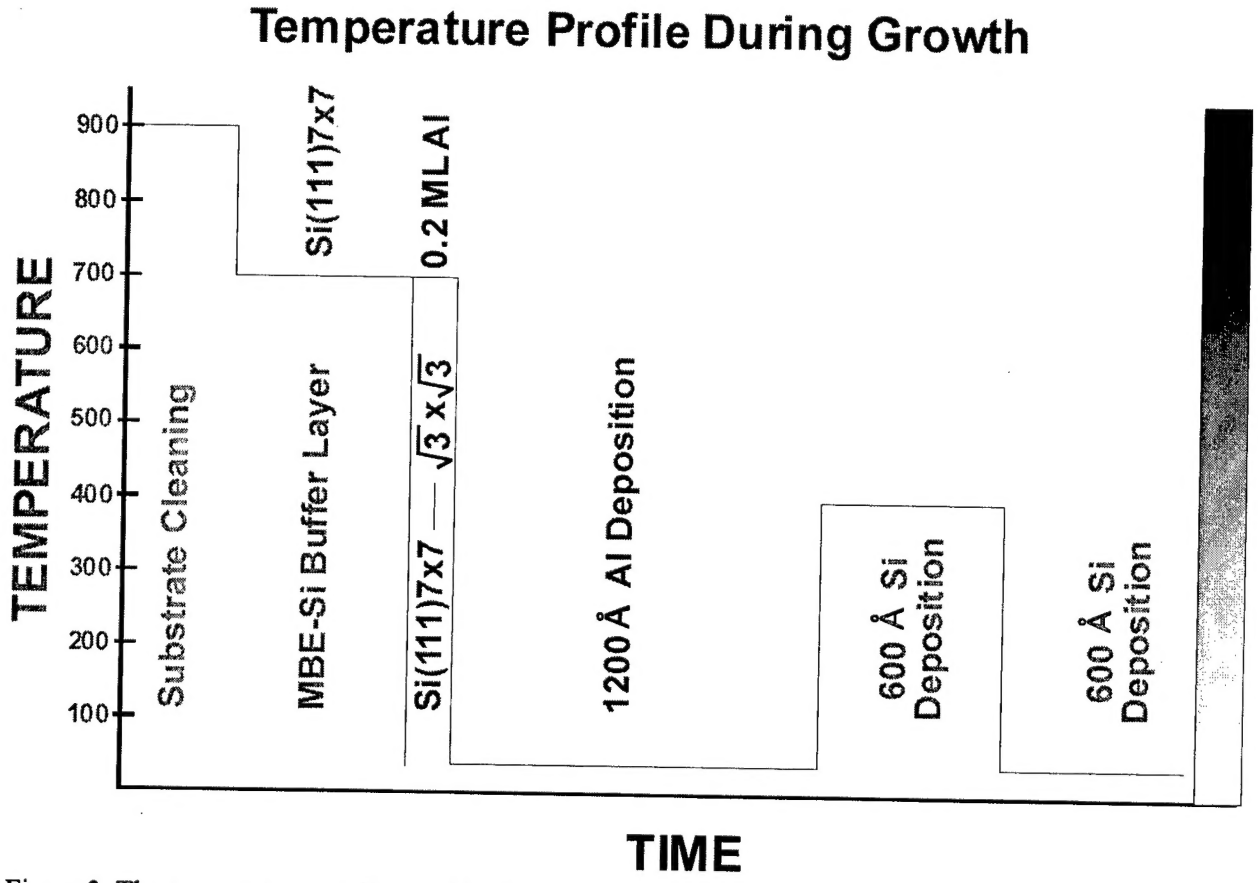

Figure 3. The temperature profile used in the current experiment.

a) after growth of the Si(111) buffer layer, the substrate temperature T_s was set to 700 °C and a 0.2 ML thick Al was grown, resulting in Al-induced Si(111)$\sqrt{3}$x$\sqrt{3}$ reconstruction. This step is a necessary surface preparation in order to establish single crystalline Al(111) layer [9].
b) T_s was reduced to room temperature (RT) and the sample was allowed to cool for one hour. A long waiting time was used to allow for the formation of a minute amount aluminum oxide. The oxide was used as a marker layer to define the buried interface (see the discussion of Figure 4).

The presence of the minute amount of the oxide was detected by SIMS measurement. Al was then deposited to a thickness of 1200 Å forming a single crystalline Al(111) layer.

c) T_S was increased to 400 ^oC and Si was deposited using a growth rate of 1 Å/s for 10 minutes.

d) T_S was reduced again to RT and a cap layer of amorphous Si was deposited using the same rate and time as in the previous layer. This layer was used as an internal reference for the SMM-MBE layer.

At the end of each of the above steps, AES and LEED were recorded. Post-deposition characterization of the samples included AES depth profiling, secondary ion mass spectrometry (SIMS), and transmission electron microscopy (TEM).

II.2. Experimental Results

Figure 4 shows a cross-sectional TEM bright field image taken from the sample described by the steps a to d above. The thickness of the top a-Si layer is 60 nm. At the original Al(111)/Si(111) interface, traces of Al oxide, due to step b, can be seen as thin platelets having a higher contrast.

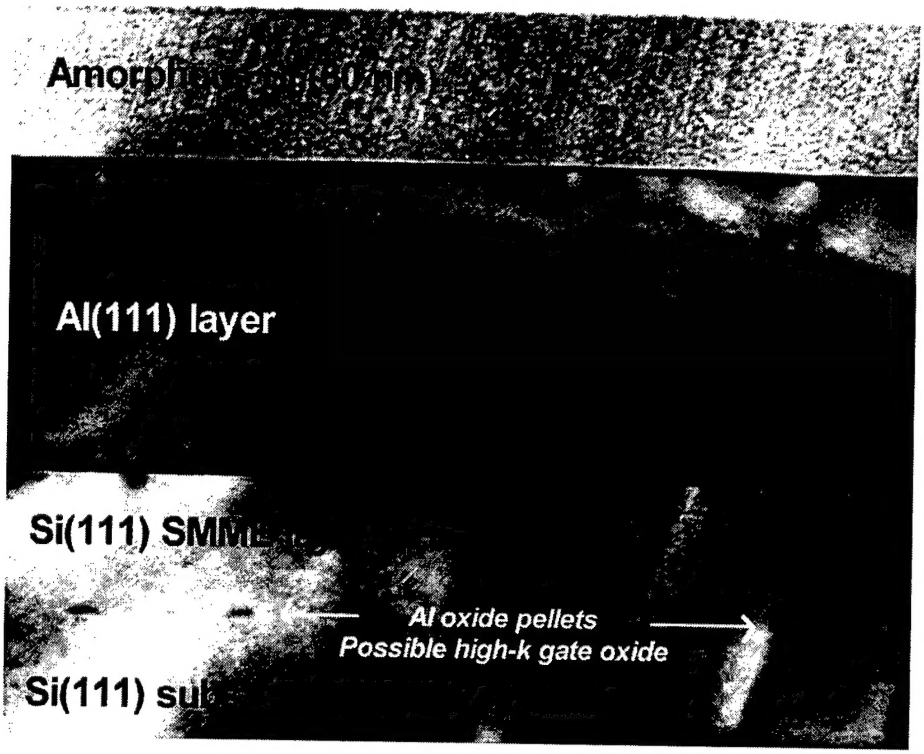

Figure 4. Bright-field transmission electron microscope image showing the resulting structure after deposition of Si by SMM-MBE and an amorphous cap layer. Note the position of the oxide particles at the original Al/Si interface (see text).

The presence of the thin oxide particles was also detected *in-situ* by AES. On top of this layer Al(111) was grown. However, the TEM image shows the Al-oxide markers are located between

two Si layers and the Al(111) layer was pushed outward by an extent equivalent to the expected thickness (~ 60 nm) of the Si layer grown at 400 °C. Thus the deposited Si in-diffused into the Al(111) layer, migrated to the Al(111)/Si(111) interface and re-grow epitaxially at the buried interface.

Remarkably, the new Al(111)/Si(111) interface is still abrupt with no measurable roughness, indicating that epitaxial growth of Si was carried out two-dimensionally via a layer-by-layer growth process. The top layer in figure 4 was grown at RT and, as expected, formed amorphous Si with pronounced columnar structure. This layer was grown to the same thickness as the SMM-MBE layer in order to provide an internal reference for the SMM-MBE layer. No apparent interdiffusion or recrystallization can be observed, indicating that the Al/a-Si interface is stable up to the highest temperature used during sample preparation, which was ~ 100 °C. The abruptness/flatness of the Al(111)/a-Si interface reflects the smoothness of the Al(111)-layer surface. Also, the smooth Al(111) surface indicates that the massive Si in-diffusion during the growth of the Si layer at 400 °C has not resulted in appreciable surface roughness. The same conclusion was also obtained from LEED which showed sharp Al(111)1x1 diffraction spots.

Figure 5 shows a TEM diffraction pattern taken from the cross-section shown in Figure 4. The diffraction pattern corresponds to fully relaxed Al(111) on Si(111) and there is no indication of any other phases or orientations. The Al diffraction is sharp indicating high quality Al(111) crystal.

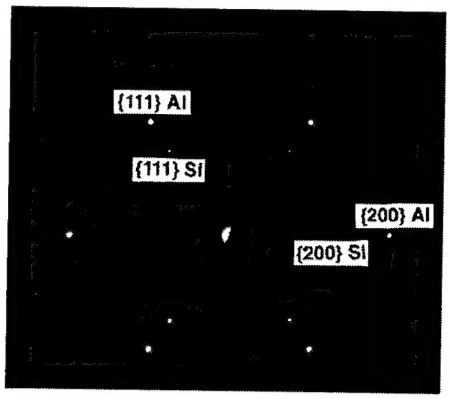

Figure 5. Selected area diffraction pattern taken from the Al/Si structure shown in Figure 4. The diffraction indicates single phase, single crystal Al and Si layers.

Figs 6 show AES spectra and LEED patterns recorded at the end of each deposition steps described in section II.1. In Fig. 6a, the AES spectrum and LEED pattern taken after thermal cleaning and deposition of the Si buffer layer are shown. Except for intense Si signal, the AES spectrum was bare of any measurable contamination peaks. The corresponding LEED pattern shows sharp and intense Si(111)7x7 reconstruction with minimal broadness and background intensity indicating highly ordered Si(111)7x7 surface with large terraces.

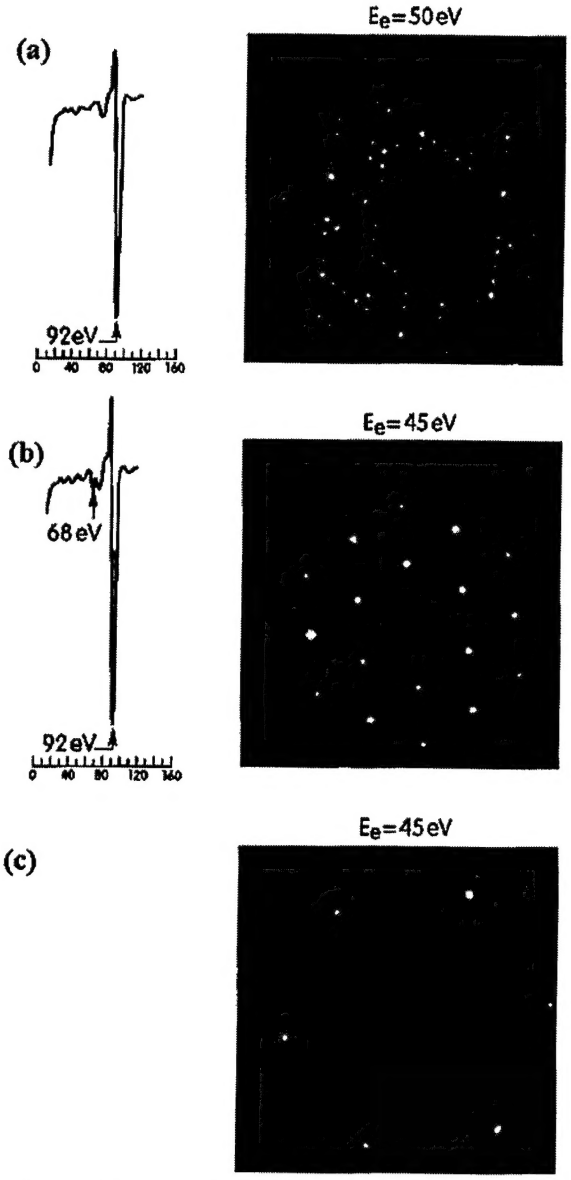

Figure 6. a) LEED and AES recorded after Si surface cleaning, b) LEED and AES after deposition of 0.2 ML of Al at 700 °C resulting in Si(111)$\sqrt{3}$x$\sqrt{3}$ surface reconstruction, and c) LEED pattern after deposition of 120 nm thick Al layer, Al(111)1x1 surface pattern is shown.

The growth of Al on a Si(111)7x7 surface typically results in the formation of two domain of epitaxial Al crystals [10]. The first is Al(111) which is the dominant structure and the second is Al(001), which comprises a minor fraction of the deposited film. In a separate study [9] we have shown that for growth at RT a single domain of Al(111) crystals can be obtained if the starting Si(111) surface is $\sqrt{3}$x$\sqrt{3}$ reconstructed instead of 7x7. Si(111)$\sqrt{3}$x$\sqrt{3}$-Al surface offer a rather simple, Al-passivated surface which can act as a straight-forward base for (111) stacking of Al. Fig. 6b shows AES and LEED pattern recorded after deposition of 0.2 ML of Al at T_S = 700 °C. It is well known that deposition of ~ 0.2-0.3 ML of trivalent metals on Si(111)7x7 surface at T_S values > 600 °C results in the establishment of Si(111)$\sqrt{3}$x$\sqrt{3}$ surface. The new reconstruction is stable and persists upon cooling to room temperature. Deposition of Al on this surface results, as mentioned above, in the formation of single domain Al(111) surface. A LEED pattern from the surface of a 1200 Å thick Al(111) layer is shown in Fig. 6c. Diffraction spots in the

unreconstructed LEED pattern are well defined and sharp, indicating a smooth Al(111)1x1 surface. Also, the background intensity is barely measurable manifesting minimal surface defects such as displaced surface atoms and screw-dislocation sites. The Al/Si epitaxial relationship reported earlier [10] can also be deduced by comparing LEED patterns of Fig. 6a and 6c.

Fig 7 shows AES and LEED results taken after growth of Si on the freshly deposited Al(111) surface at 400 °C. Si growth rate was 1 Å/s. The dominating AES signal is still Al LMM at 68 eV with a barely measurable Si signal. In addition, the LEED diffraction pattern, except for a slightly higher background intensity, was the same as in Fig. 6c which was taken after initial deposition of the Al layer. These results are consistent with the TEM results and indicate Si in-diffusion into the Al(111) layer.

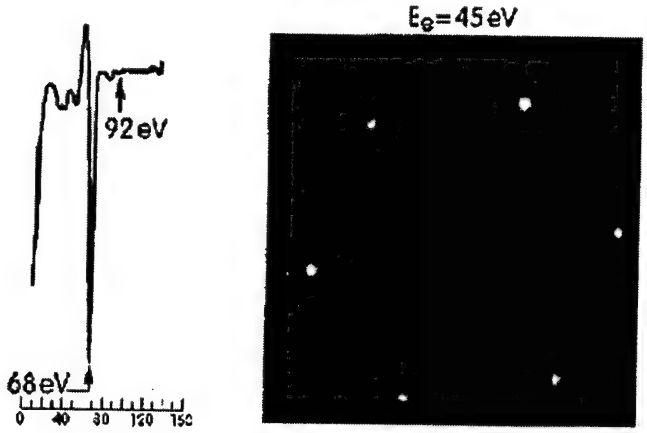

Figure 7. LEED and AES recorded after deposition of 60 nm thick Si layer at 400 °C. No traces of Si could be recorded.

In order to have an internal reference for the thickness of the SMM-MBE layer, a Si cap layer was deposited at room temperature using deposition rate and time equal to that used for the previous layer. AES from the RT-deposited Si layer is shown in Fig. 8. There is no measurable Al signal in this case.

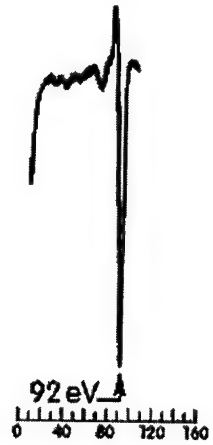

Figure 8. AES spectrum from the a-Si top layer. Only the Si signal present and no traces of Al.

Figure 9 shows AES depth profile for the same sample. The Figure shows, consistent with the TEM results, a sharp transition at the Al/Si interfaces. The slight increase in the width of the Al/Si interface with increasing depth is due to increase in the sampling width caused by the

increased roughness of the sputtering front at higher crater depths. Collisional mixing induced by the sputtering gas atoms (Ar in this case) will also add to the measured broadening. The concentration of Si in the Al layer and of Al in the Si layer were below the AES elemental resolution limit. For the same reason, the presence of the marker layer was not detected. However, SIMS clearly showed the presence of a minute amount of oxygen at the interface between the SMM-MBE Si layer and the substrate.

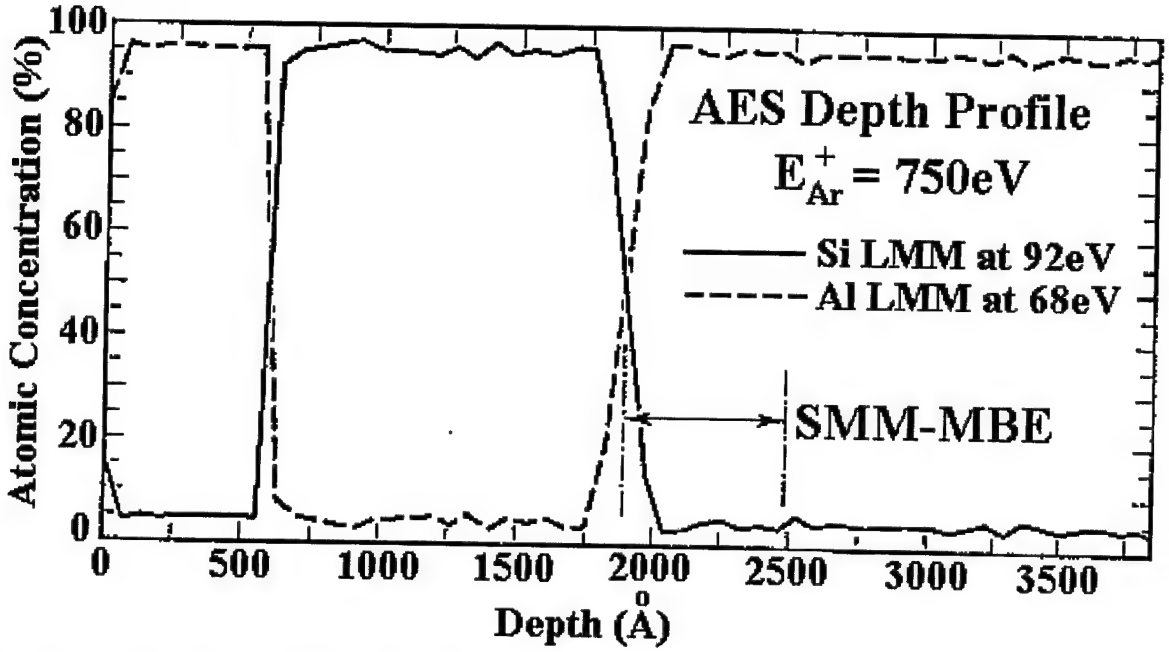

Figure 9. AES depth profile taken from the same structure.

III. SMM-MBE ON Si(100)

SMM-MBE growth on Si(100) was conducted following similar procedures to that described in Sec. II.1 with the exception of surface-reconstruction induced epitaxy (SRIE).

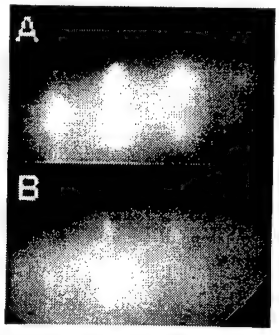

Figure 10. RHEED patterns taken: (A) after deposition of Al on Si(100). The diffraction demonstrates the growth of single crystalline Al layer. (B) after deposition of Si on the Al layer. The only observable diffraction pattern is that of Al indicating absence of Si on the surface. The Si layer regrew at the buried Al/Si interface. The sample in B is slightly rotated resulting in the change in the relative intensities of diffraction spots.

Figure 10 shows RHEED pattern taken from SMM-MBE growth at 300 °C. In Figure 10A, the diffraction from a single crystalline Al layer grown on Si(100) at room temperature is shown. In Figure 10B, the diffraction is taken after heating the sample to 300 °C and deposition of Si. Except

for a higher background intensity due to greater surface disorder and a change in the relative intensity of the diffraction spots due to slight rotation of the sample, there is no measurable diffraction from other phases or materials. Similar to the case of growth on Si(111), the deposited Si diffused through the Al overlayer and regrew at the buried interface.

IV. Growth of Si on Insulators (SOI) using SMM-MBE

In addition to growth on non-patterned plane surfaces, we have carried out some experiments to demonstrate the capabilities of SMM-MBE in direct integration with CMOS fabrication (highly doped shallow source/drain structures) and extension to SOI layers. The basic idea is to utilize lateral epitaxial overgrowth on a patterned surface as shown in Figure 11. An oxide layer is patterned on the surface leaving single crystalline Si seed in between. Al is then deposited first followed by Si. The structure can be used for shallow junction source/drain fabrication (by slightly etching the Si surface between the oxide islands (gate oxide) as well as for SOI fabrication.

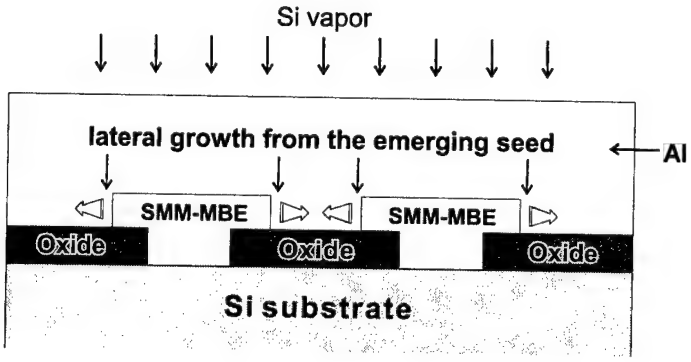

Figure 11. Schematic showing the mechanism of lateral growth on the oxide features during SMM-MBE.

To demonstrate these possibilities, we have utilized a special mask with five areas on the wafer (see Fig. 12). Each area is patterned with a fixed seed to oxide widths. With this configuration multiple seed/oxide configurations can be examined simultaneously. In addition the dependence lateral overgrowth on the crystallographic orientation of the seed area can be investigated by rotating the mask with respect to the wafer.

RHEED pattern from a sample grown using this method is shown in Figure 13. The RHEED pattern indicates growth of polycrystalline Al on the patterned surface. This is expected since the oxide layer is amorphous and does not provide a template for single crystalline growth. The pattern stay the same after deposition of Si on the surface indicating growth of the Si at the buried surface.

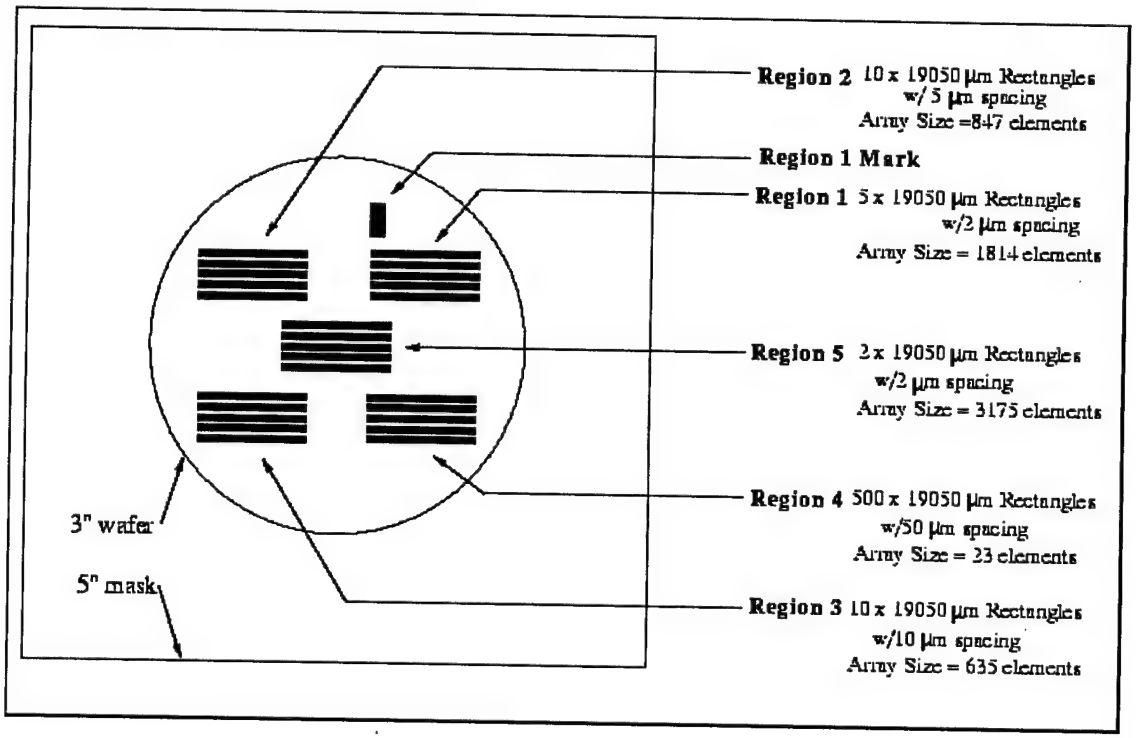

Figure 12. The mask used to investigate the dependence of SMM-MBE lateral epitaxial overgrowth on seed/oxide dimensions and orientation. Each area has a fixed seed/oxide dimension.

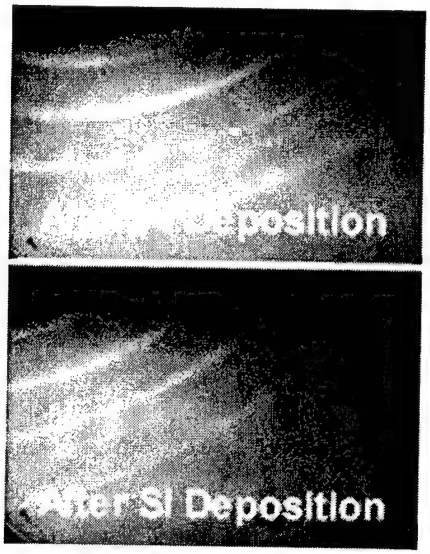

Figure 13. RHEED pattern after growth of Al on patterned Si surface. Polycrystalline is expected due to the presence of SiO_2. The pattern stays the same after growth of Si at 400 °C indicating growth of Si at the buried interface.

In order to better understand the growth, lateral epitaxial overgrowth (LEO) was examined by transmission electron microscope (TEM). Figure 14 shows a cross-sectional TEM image from a Si layer grown on a SiO_2 strip patterned according to the procedure described above. The

overlayer Si shows no indication of dislocations or grain boundary formation indicating high quality growth of Si on the oxide layer.

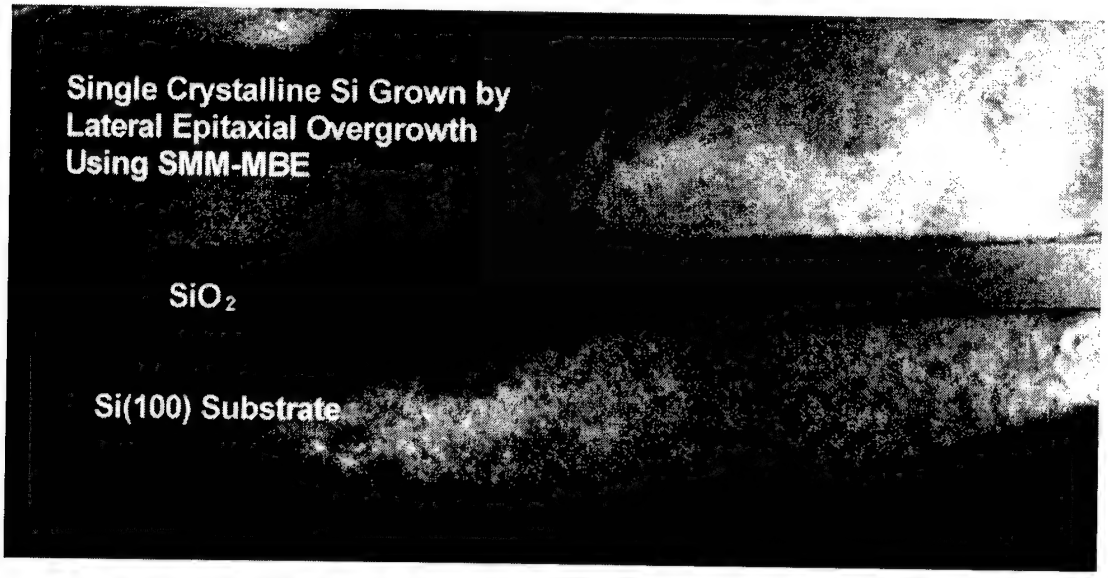

Figure 13. Cross-sectional TEM showing LEO of Si on oxide using SMM-MBE. No dislocations or grain boundaries can be seen in the Si overlayer.

V. Doping of Si using SMM-MBE

Doping in the SMM-MBE comes naturally since Al is a p-type dopant in Si. As the Si grow at the buried interface, it incorporates some Al atoms during the growth. Since the growth temperature is low (<400 °C), the concentration of Al obtained is typically above the solid solubility limit. Figure 14 shows a typical SIMS doping profile obtained from a 100 nm layer grown by SMM-MBE. The maximum doping density obtained is much higher than reported solid solubility. The broadening on the profile on the substrate side is ~ 24 nm/decade, which is close to the resolution limit of SIMS. The thickness of the layer can be controlled accurately by the deposition time (amount of deposited Si).

In summary, we have demonstrated the possibility of fabricating highly doped thin layers of Si using SMM-MBE. In addition, single crystalline growth over oxide was also demonstrated, which enable integration of SMM-MBE with CMOS processing as well as limited area SOI growth.

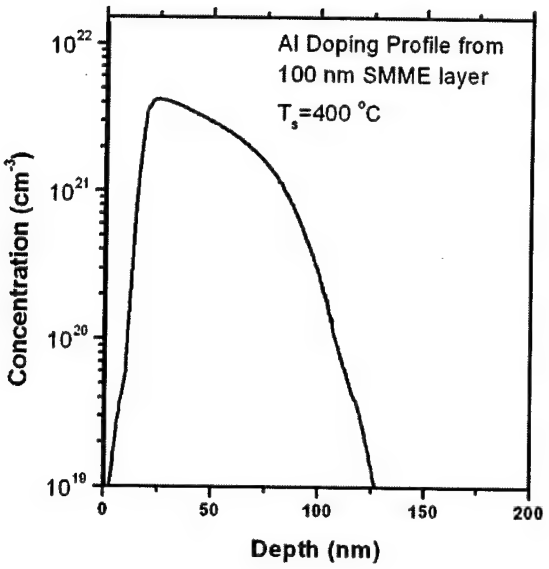

Figure 14. SIMS profile from a 100 nm thick Si layer grown by SMM-MBE. The achieved doping density is much higher than the solid solubility limit.

VI. Growth Mechanism

The growth mechanism can be understood in terms of the low solid solubility of Si in Al, the absence of Al/Si compounds, high diffusion rate of Si in Al, and low-energy Si lattice sites provided by the buried Si(111) surface. Figure 15 shows a schematic demonstrating the growth mechanism. Si deposition on the Al(111) free surface results in high concentration of Si on the Al surface. Diffusion of Si is then driven by the concentration gradient created by the deposition. As Si atoms reach the buried Si(111) surface, they encounter a low free-energy lattice-sites, occupy them and become part of the Si substrate. The incorporation of Si atoms at the substrate lattice sites results in a depletion of Si concentration near the Al/Si interface. The resulting concentration gradient drives more Si atoms toward the interface. This process continues until the Si deposition is terminated (concentration instabilities are removed). Thus, two basic processes control the growth rate at the buried interface, the diffusion rate through the Al layer and the accommodation rate as shown in Fig. 15. Clearly, intermetallic compound formation must be avoided in the mediating metal layer. Otherwise, the Si will be consumed for compound formation as in the case of silicide growth. The absence of Al silicides is thus an important condition for a successful SMM-MBE growth. Moreover, the solid solubility of Si in Al must be low enough in order to prevent alloy formation with a high Si content. Solid solubility of Si in Al is 0.05 at% at 300 oC [11]. Finally, a high diffusivity of Si in Al is needed for efficient mass transport through the Al layer. The latest condition is well supported by published diffusivity data. Pacagnalla et. al.(12) report an activation

energy for diffusion Ed = 0.8 eV and a pre-exponential factor Do = 8.3x10-3 cm2s-1 which result in an average root mean square diffusion length ($\bar{x} = \sqrt{2Dt}$) of 1300 nm for t = 1s.

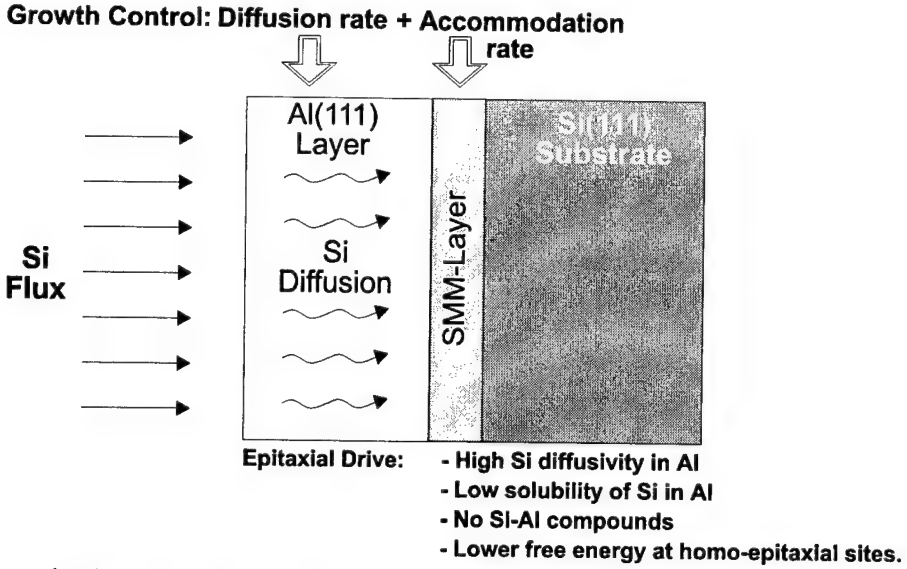

Figure 15. Schematic showing the basic processes during SMM-MBE.

These numbers are consistent with the present experimental finding. On the other hand, the solid solubility of Al in Si, even at the eutectic temperature (577 oC), is only 0.007 at% (11) while Ed = 3.2 eV [13]. These numbers explain the low concentration of Al in the SMM-MBE Si layer.

REFERENCES

1. R.S. Wagner and W. C. Ellis, Applied Phys. Lett, 4, 89 (1964)
2. R.S. Wagner and W. C. Ellis, Trans. Metall. Soc. AIMS 233, 1053 (1965)
3. F. Xiong, E. Ganz, A. G. Loeser, J. A. Golovchencho, and F. Spaepen, Appl. Phys. Lett, 59, 3586 (1991).
4. G. Majni and G. Ottaviani, Appl. Phys. Lett. 31, 125 (1977)
5. B-Y. Tsaur, G. W. Turner, and J. C. Fan, Appl. Phys. Lett. 39, 749 (1981)
6. S. S. Lau, Z. L. Liau and M.-A. Nicolet, Thin Solid Films 47, 313 (1977)
7. G. L. Olson and J. A. Roth, Mat. Res. Rep., 3, 1 (1988) and references therein.
8. R. E. Hummel and I. Yamada, Appl. Phys. lett. 54, 18 (1989)
9. M.-A. Hasan, J.-E. Sundgren and J.E. Greene, unpublished.
10. M.-A. Hasan, G. Radnoczi and J.-E. Sundgren. Vacuum, 41, 1121 (1990)
11. See for example, Binary Alloy Phase Diagram, T. B. Massaleski (ed.), American Society for Metals, Ohio, USA (1986) and Constitution of Binary Alloys, M. Hansen, McGraw Hill, NY (1958)

12. A. Paccagnella, G. Ottaviani, P. Fabbri, G. Queirolo, Thin Solid Films, 128, 217 (1985)
13. W. Rosnowski, J. Electrochem. Soc. 125, 957 (1978)

APPENDIX A

SYSTEM CONFIGURATION

1. An integrated, hybrid, gas-source MBE (GS-MBE)/solid source MBE (SS-MBE) facility (see Figure 1). The growth system, which was made by Vacuum Generators (VG Scientific), consists of four interconnected sections:

a. two MBE/GS-MBE chambers fitted with three electron beam evaporators and effusion cells,

b. analysis, and

d. two load-lock chambers (only one is shown in the Figure 1.).

This configuration of the cluster MBE/GS-MBE facility combines the advantages of SS-MBE and GS-MBE (materials choice, temperature consideration, conformal growth, etc.). The SS-MBE growth chambers, which are shielded by a liquid nitrogen shroud, contain electron beam evaporators and provisions for up to four effusion cells, gas-source or solid-source low-energy ion guns. Each electron gun, made by Airco Temscal, is provided with a dual quartz microbalance for thickness measurements and deposition control, a pneumatic shutter, and an independent view port with shutter assembly to prevent deposition on the window. The chambers are also equipped for mass-spectrometry and provisions for reflection high energy electron diffraction (RHEED). The chambers have many additional ports that allow expansion of the system and the addition of other surface processing and characterization techniques. The facility is pumped by a combination of turbo pump, Cryo and titanium sublimation pumps unit while roughing is accomplished by using a root/mechanical pumping station. The Deposition chamber I, which is also cooled by a LN2 shroud, equipped for up to eight materials delivery sources and provisions for RHEED, mass-spectrometry, and thickness monitor. In addition, it can accommodate a 40cc or two smaller electron guns. The analysis chambers contain provisions for Auger electron spectroscopy (AES) and low-energy electron diffraction (LEED). AES utilizes a CLAM2 hemispherical analyzer made by VG which is also capable of XPS/UPS measurements. An ion source is also available for surface cleaning and AES depth profiling. The computerized CCD-LEED/RHEED vision and profiling system will provide a detailed correlation of diffraction spots' profiles versus the surface domain sizes, roughness and reconstruction. The three load-locks, which are pumped independently, can handle sample magazines with up to ten samples at each load-lock station.

The system base pressure is $\sim 5 \times 10^{-11}$ Torr. The facility can handle up to 3" wafers in two of the deposition chambers and up to 4" in the third chamber. Also, it can be modified to handle up to 6" wafers.

A schematic of the system is shown in Figure 1.

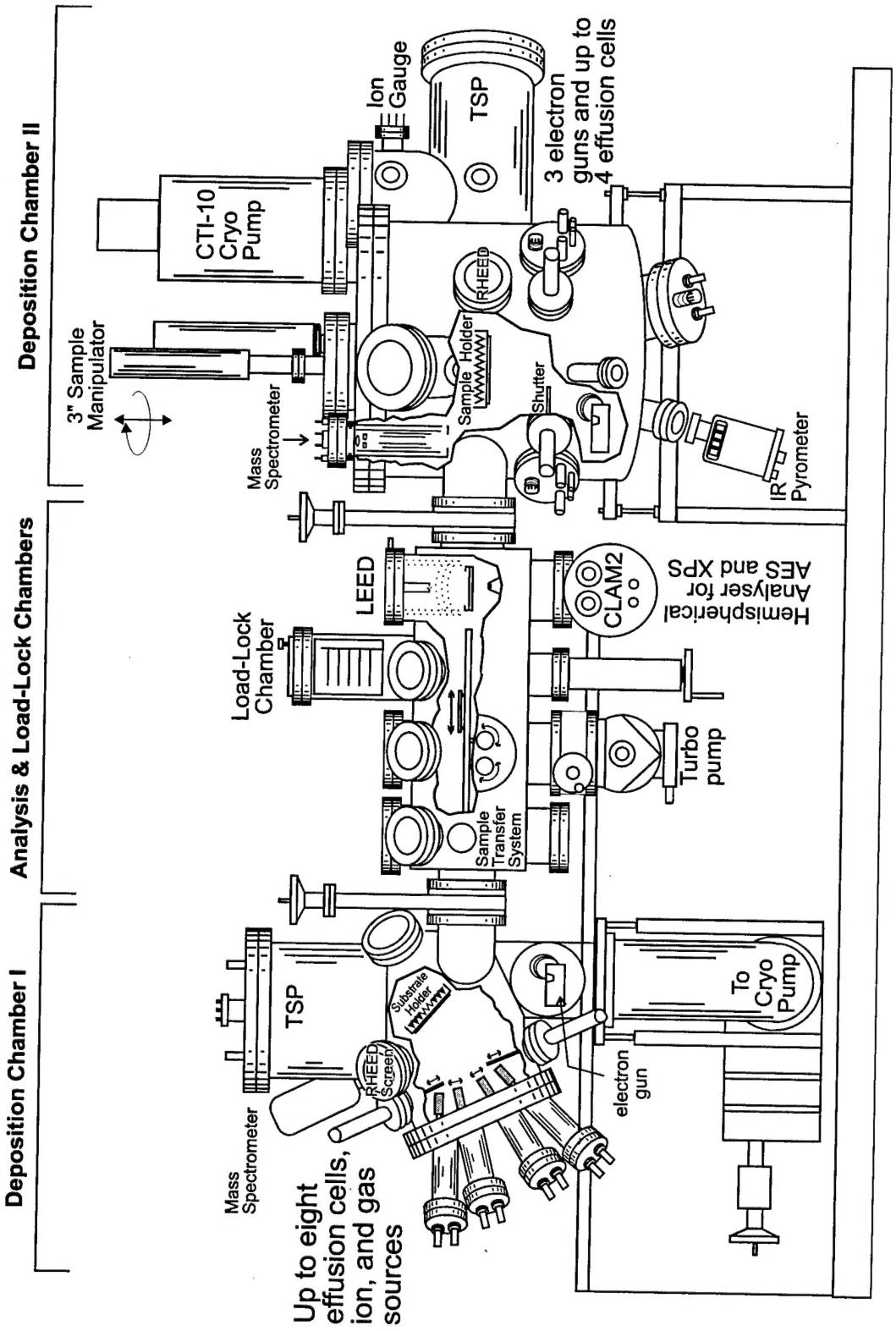

Figure 1. A schematic of the GS-MBE/SS-MBE described in the text. The third chamber and its analysis section are not shown.

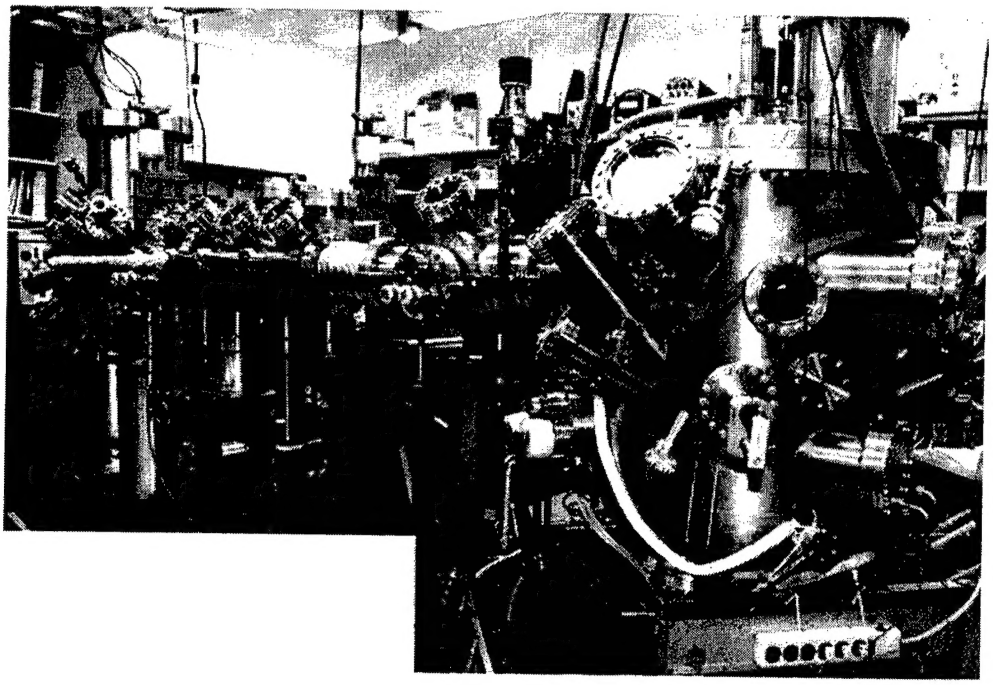

Figure 2 (a above and b below). Side views of the growth facility.